The BLOC-1 complex promotes endosomal maturation by recruiting the Rab5 GTPase-activating protein Msb3

Arun T. John Peter, Jens Lachmann, Meenakshi Rana, Madeleine Bunge, Margarita Cabrera, and Christian Ungermann

Department of Biology/Chemistry, Biochemistry Section, University of Osnabrück, 49076 Osnabrück, Germany

Membrane microcompartments of the early endosomes serve as a sorting and signaling platform, where receptors are either recycled back to the plasma membrane or forwarded to the lysosome for destruction. In metazoan cells, three complexes, termed BLOC-1 to -3, mediate protein sorting from the early endosome to lysosomes and lysosome-related organelles. We now demonstrate that BLOC-1 is an endosomal Rab-GAP (GTPase-activating protein) adapter complex in yeast. The yeast BLOC-1 consisted of six subunits, which localized interdependently to the endosomes in a Rab5/Vps21-dependent manner. In the absence of BLOC-1 subunits, the balance between recycling and degradation of selected cargoes was impaired. Additionally, our data show that BLOC-1 is both a Vps21 effector and an adapter for its GAP Msb3. BLOC-1 and Msb3 interacted in vivo, and both mutants resulted in a redistribution of active Vps21 to the vacuole surface. We thus conclude that BLOC-1 controls the lifetime of active Rab5/Vps21 and thus endosomal maturation along the endocytic pathway.

Introduction

Endocytosis of plasma membrane proteins begins with their packaging into endocytic vesicles, which fuse with the early endosome. At the early endosome, the fate of the internalized cargo protein is decided. Cargo receptors such as the LDL (low density lipoprotein) receptor are sorted into membrane domains on the early endosomes that are eventually separated from the endosome and brought back to the plasma membrane. Other receptors or transporters are marked for destruction and remain on the early endosome, which then matures into the late endosome (Huotari and Helenius, 2011). During the maturation process, the receptors are sorted into the lumen of the late endosome, a process orchestrated by the ESCRT complexes leading to the formation of a multivesicular body (MVB; Henne et al., 2011). Upon completion, MVBs fuse with lysosomes, and receptors are degraded by lysosomal hydrolases. Importantly, the maturation event is accompanied by a change in the fusion machinery on the surface of endosomes (Huotari and Helenius, 2011). Whereas early endosomes carry the Rab5 GTPase, late endosomes/MVBs harbor the Rab7 GTPase (Rink et al., 2005; Poteryaev et al., 2010; Huotari and Helenius, 2011). For fusion, Rabs in their GTP form bind tethering factors, which promote membrane contact and support the SNARE-driven mixing of lipid bilayers. During endosomal maturation, the yeast Rab5-like Vps21-GTP seems to be linked to the recruitment of the Mon1–Ccz1 guanine nucleotide exchange (GEF) complex, which then activates the yeast Rab7-like Ypt7 (Nordmann et al., 2010). Recent studies showed that the Msb3 GTPase-activating protein (GAP) subsequently inactivates Vps21, thus maintaining organelle identity along the endolysosomal pathway (Lachmann et al., 2012; Nickerson et al., 2012). Msb3 function is thus similar to mammalian RabGAP-5, which regulates endocytic transport via its action on Rab5 (Haas et al., 2005). However, the temporal and spatial coordination of Vps21 inactivation reaction remains unclear.

Several protein complexes are involved in cargo sorting and biogenesis of the early endosome. In addition to Rab5 that operates in endosomal fusion, sorting nexins and the retromer complex mediate the recycling of receptors back to the Golgi or

Correspondence to Margarita Cabrera: Margarita.Cabrera@biologie.uni-osnabrueck.de; or Christian Ungermann: Christian.Ungermann@biologie.uni-osnabrueck.de

Abbreviations used in this paper: GAP, GTPase-activating protein; GEF, guanine nucleotide exchange; TYRP, tyrosinase-related protein.

The Rockefeller University Press $30.00
J. Cell Biol. Vol. 201 No. 1 97–111
www.jcb.org/cgi/doi/10.1083/jcb.201210038

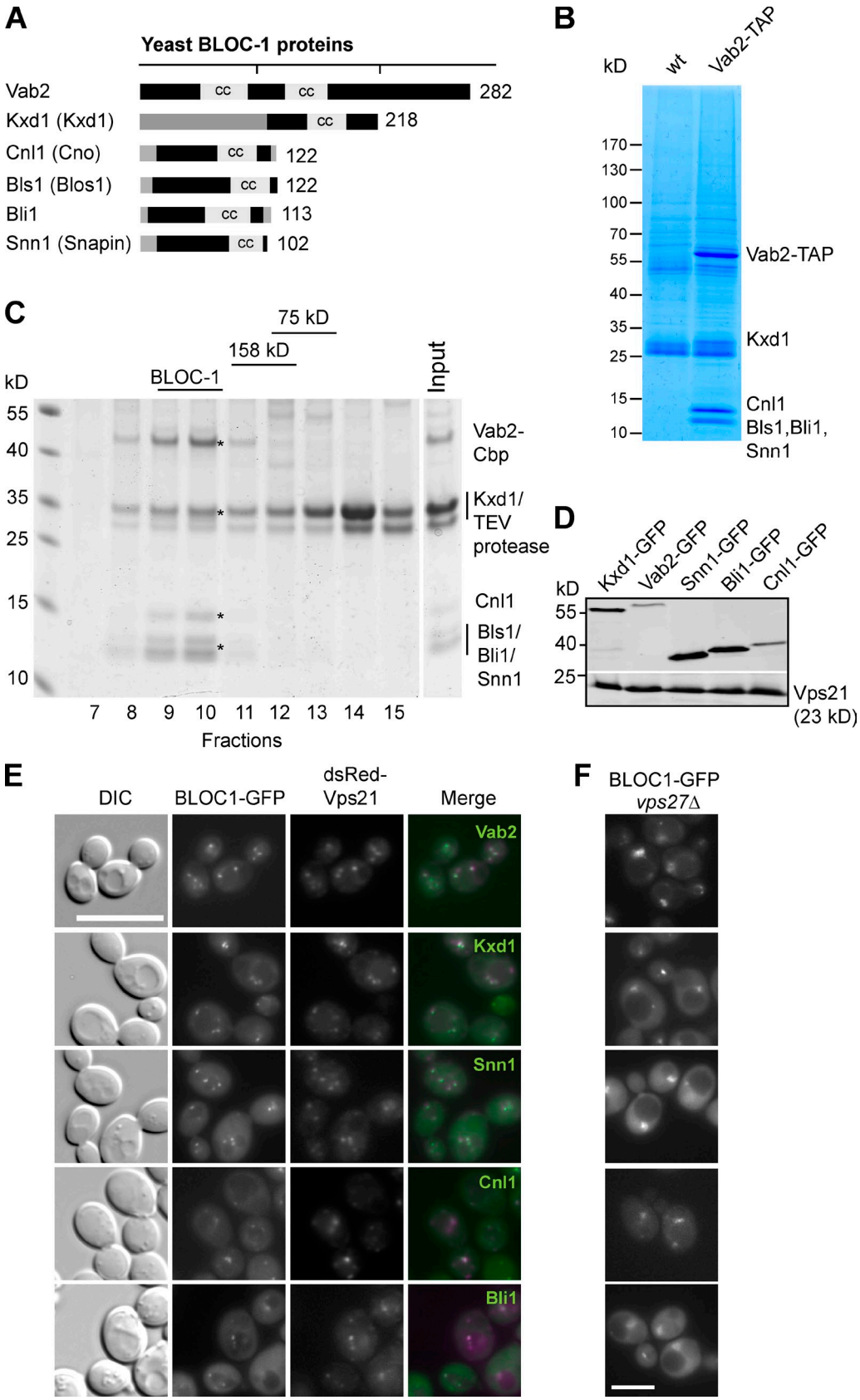

Figure 1. **Identification of the BLOC-1 complex.** (A) Subunits of the yeast BLOC-1 complex. The number of amino acid residues are indicated for each subunit. The ruler has marks at each 100 residues. Mammalian subunits are shown in brackets. Black indicates α-helical regions, cc stands for predicted coiled-coil domains as determined by Predict Protein (www.predictprotein.org) and the coiled-coil prediction program (http://toolkit.tuebingen.mpg.de/pcoils). (B) Isolation of the overexpressed BLOC-1 complex. Vab2 was purified via its C-terminal TAP tag from a diploid strain with all subunits under

the plasma membrane (Bonifacino and Hurley, 2008; Cullen, 2008). Although these sorting and fusion factors are conserved also in lower eukaryotes, endosomal BLOC complexes have been assigned primarily to metazoans. The three identified BLOC complexes have been linked to the Hermansky-Pudlak syndrome (HPS), an inherited disease characterized by defects in skin pigmentation and blood clotting (Dell'Angelica, 2004; Wei, 2006). BLOC-1 to -3 presumably act consecutively and are required for the biogenesis of melanosomes (Raposo and Marks, 2007; Dell'Angelica, 2009). BLOC-1 is a hetero-octamer (Lee et al., 2012), which cooperates with the AP-3 complex in neuronal cells (Salazar et al., 2006; Newell-Litwa et al., 2009), localizes to early endosomal tubules (Di Pietro et al., 2006), and is required for sorting of tyrosinase-related protein 1 (TYRP1) to melanosomes (Di Pietro et al., 2006). Overall, its eight subunits (dysbindin, cappuccino, muted, pallidin, snapin, and BLOS1, -2, and -3) seem to be predominantly α-helical in structure, and have several interaction partners, including SNAREs (Rodriguez-Fernandez and Dell'Angelica, 2009). Consistent with the structure prediction, the recombinant mammalian BLOC-1 forms a linear chain of eight associated subunits as revealed by electron microscopy (Lee et al., 2012). Recently, KXD1 was identified as a novel metazoan BLOC-1 subunit (Yang et al., 2012), and has a homologue in yeast (Hayes et al., 2011). BLOC-2 (with its subunits Hps3, -5, and -6; Gautam et al., 2004; Di Pietro et al., 2004) and BLOC-3 (Hps1 and -4; Martina et al., 2003; Nazarian et al., 2003; Kloer et al., 2010) then potentially act downstream of BLOC-1 to enable proper cargo sorting (Raposo and Marks, 2007; Gerondopoulos et al., 2012).

Mutations in the BLOC genes lead to defective cargo trafficking to lysosome-related organelles, which eventually results in coat color alterations and excessive bleeding in mice (Gautam et al., 2004; Wei, 2006), and defective eye pigmentation in *Drosophila* (Cheli et al., 2010). Among the known genes mutated in HPS, mutations in five of the eight BLOC-1 genes manifest the disease phenotype in mice (Yang et al., 2012). Moreover, the human BLOC-1 subunit dysbindin, *DTNBP-1*, has been linked to schizophrenia (Straub et al., 2002; Ghiani and Dell'Angelica, 2011; Mullin et al., 2011), suggesting defects in protein trafficking in the affected neurons. Although the disease phenotypes associated with BLOC-1 mutations appear to be cell type specific, BLOC-1 complex is ubiquitously expressed (Wei, 2006), suggesting that, in nonspecialized cells, it may also carry out sorting functions and maintain the integrity of the endolysosomal pathway.

Despite the wealth of in vivo studies, little is known about the precise molecular function of BLOC-1 at endosomes. A recent bioinformatics study by Levine and coworkers provided evidence that BLOC-1 may also exist in yeast, suggesting that BLOC-1 may be a general sorting factor of eukaryotic cells that is not restricted to lysosome-related organelles (Hayes et al., 2011). The authors identified six interacting subunits based on homology search, and published large-scale yeast two-hybrid and proteomics studies (Krogan et al., 2006). This was recently confirmed by another large-scale proteomics study on yeast membrane proteins (Babu et al., 2012). One of the subunits of the proposed complex is Vab2, an interactor of the vacuolar fusion factor Vac8 (Pan et al., 2000). Within this study, we now reveal that the Vab2-containing BLOC-1 complex regulates the transport of cargo through the endocytic pathway, and serves as the receptor of the Msb3 GAP protein to promote endosomal maturation.

Results

Yeast BLOC-1 is an endosomal complex

Bioinformatic analyses suggested the presence of a hexameric BLOC-1 complex in yeast (Hayes et al., 2011). The proposed yeast BLOC-1 complex has six subunits with predicted α-helical secondary structure, and several coiled-coil domains (Fig. 1 A). It was, however, unclear if all subunits are indeed part of a complex. We previously learned that efficient purification of large complexes requires a simultaneous overexpression of all subunits (Ostrowicz et al., 2010; Bröcker et al., 2012). We used the same approach to test if the six subunits form the yeast BLOC-1. When we then purified the complex via tagged Vab2, using the tandem affinity tag protocol (Ostrowicz et al., 2010), we obtained six subunits on Coomassie-stained gels, which were identified by mass spectrometry as the predicted six BLOC-1 subunits (Fig. 1 B), in agreement with the recent findings of Babu et al. (2012). To confirm further that the co-eluted subunits are part of a stable complex, we applied the purified BLOC-1 complex onto a Superose 12 column and analyzed the eluted fractions. Indeed, all six subunits were found as a complex with an approximate molecular weight of 158 kD (Fig. 1 C). This led us to hypothesize that the subunits of the BLOC-1 complex might localize to the same intracellular compartment. To address this, all the subunits except Bls1 were C-terminally tagged with GFP, and subsequently localized by fluorescence microscopy. We also observed that Vab2 and Cnl1 were less expressed than the other subunits (Fig. 1 D) and that the tagging did not interfere with function of the subunits (see Fig. 4 D). As mammalian BLOC-1 is found on endosomes, we decided to follow dsRed-tagged Vps21 in parallel, and indeed observed colocalization with Vps21 to dot-like structures, even though a large portion of the BLOC-1 subunits was found in the cytosol (Fig. 1 E). We therefore asked if the localization of BLOC-1 to endosomes could be enhanced in mutants lacking Vps27, a subunit of the ESCRT

the control of the *GAL1* promoter. Coomassie-stained proteins that co-purified with Vab2 were identified by mass spectrometry. For details, see Materials and methods. (C) Size-exclusion chromatography of the BLOC-1 complex. BLOC-1 complex purified via the TAP-tagged Vab2 was eluted from the IgG Sepahrose beads using TEV protease. The eluted complex, standard proteins conalbumin (158 kD), and aldolase (75 kD) were loaded onto a Superose 12 column. Fractions were TCA precipitated, loaded onto SDS-PAGE gels, and stained with Coomassie. (D) Expression of all BLOC-1 subunits. GFP was added C terminally. Cell extracts were loaded onto gels, blotted, and decorated with antibodies against Vps21 and GFP. (E) Colocalization of BLOC1 subunits with Vps21. Cells expressing the GFP-tagged BLOC-1 subunits and dsRed-tagged Vps21 from a CEN plasmid were analyzed by fluorescence microscopy. Bar, 5 µm. (F) Localization of BLOC-1 subunits in the absence of ESCRT-0 subunit Vps27. The respective deletion strains were analyzed by fluorescence microcopy. Bar, 5 µm.

complex. ESCRTs are required to channel membrane proteins into intraluminal vesicles (Henne et al., 2011). In the absence of this complex, many endosomal proteins accumulate in an enlarged membrane compartment proximal to the vacuole. This also applied to all analyzed BLOC-1 subunits (Fig. 1 F), suggesting that BLOC-1 is indeed an endosomal protein complex.

Endosomal localization of BLOC-1 requires the entire complex and the Rab5 homologue Vps21

We then asked if the localization of the BLOC-1 subunits is interdependent, and therefore localized them in the absence of the other subunits. Surprisingly, the clear endosomal localization was lost in almost every deletion strain (Fig. 2 A). Only Vab2-GFP seemed to be present in some puncta when Snn1 was deleted, though these were less pronounced than in wild-type cells. In addition, Vab2 was also found on vacuoles in some deletions, in agreement with its binding to the vacuolar Vac8 protein (Pan et al., 2000). To rule out that the mislocalization observed in BLOC-1 mutants was due to the absence of endosomes, we localized the endosomal SNARE Pep12 and found that the endosomal identity was maintained in *kxd1Δ* cells (Fig. 2 B). Consistent with the codependent localization of the subunits, the interaction between Snn1-GFP and Vab2-HA was lost if the Bli1 subunit was absent (Fig. 2 C), indicating that the BLOC-1 subunits associate as a complex with endosomes.

We expected that endosomes have a conserved recruitment factor for BLOC-1. The Rab5 homologue Vps21 is critical for the localization of several endosomal proteins including Vps34, the phosphoinositol-3 kinase (Schu et al., 1993), and the CORVET tethering factor (Cabrera et al., 2012). As three Rab5 homologues (Vps21, Ypt52, and Ypt3) exist in yeast, we localized the BLOC-1 subunit Snn1-GFP in single, double, and triple deletions, and observed strong mislocalization of the protein to the vacuole rim in the *vps21Δ* mutant (Fig. 3 A). The extent of mislocalization did not get enhanced in the triple deletion strain of endosomal Rabs. Interestingly, deletion of the Rab7 homologue Ypt7, the terminal Rab of the endolysosomal pathway, did not affect the endosomal localization of Snn1. A similar phenotype resulted upon deletion of class D genes such as *VPS45* and *VAC1* (Fig. 3 A), indicating that the loss of endosomal localization was specific for Vps21. We also tested the other BLOC-1 subunits and observed a similar mislocalization upon loss of Vps21, except that Bli1 and Cnl1 were mostly cytosolic (Fig. 3 B). This localization data agreed with previous findings that Snn1 and Kxd1 directly interact with Vab2, as discussed in Hayes et al. (2011), and hence, in *vps21Δ* cells, these subunits might end up at the vacuole due to the interaction between Vab2 and Vac8. To confirm whether the vacuolar redistribution of BLOC-1 in the *vps21Δ* mutant depends on Vac8, we localized Snn1 and observed a complete cytosolic localization in the *vps21Δ vac8Δ* double deletion strain. Furthermore, deletion of *VAC8* alone did not affect the subcellular distribution of Snn1 (Fig. 3 C).

To directly test if BLOC-1 binds Vps21 as an effector, we added purified BLOC-1 to GST-tagged Vps21, Ypt7, and Ypt1 that were preloaded with GTPγS or GDP. When we analyzed the bound protein fractions, we found that BLOC-1 subunit Vab2 preferentially associated with Vps21-GTP (Fig. 3 D). Taken together, our data show that activated Vps21 is a major factor involved in the recruitment of BLOC-1 to endosomes.

As we realized that Vps21 is critical for endosomal localization of the complex, we wondered whether BLOC-1 assembly requires Rab5 activity. Therefore, we followed the interaction between Snn1-GFP and Vab2-TAP in the wild-type and the triple Rab deletion strain, which allows to rule out functional compensation by the Vps21 homologues. Interestingly, the interaction could be observed even in the absence of the endosomal Rabs (Fig. 3 E), indicating that the BLOC-1 assembly is likely to be a Rab-independent event.

BLOC-1 regulates cargo recycling to the plasma membrane

In mammalian cells, BLOC-1 is responsible for the sorting of TYRP1 from early endosomes to melanosomes (Di Pietro et al., 2006). As specialized lysosome-related organelles do not seem to exist in yeast, we speculated that the complex might be involved in the trafficking of cargo along the endocytic pathway. However, none of the BLOC-1 mutants showed any obvious defect in assays monitoring the sorting of Golgi-derived cargo (GFP-Cps1), endocytic cargo (Ste3-GFP) to the vacuole lumen, the retromer-mediated recycling of receptors at the late endosomes (Vps10-GFP), the Snx complex–mediated recycling of Snc1 (GFP-Snc1), and the recycling of the calcium-dependent serine protease Kex2 (Fig. 4 A). Unlike in the mammalian context, where BLOC-1 affects the trafficking of the AP-3 cargo such as LAMP1 (Salazar et al., 2006), yeast BLOC-1 mutants had no effect on the sorting of the AP-3 cargo GNS (GFP–Snc1–Nyv1 fusion; Fig. 4 A; Reggiori and Pelham, 2001). Likewise, general endocytic transport and selective autophagy, monitored by CPY secretion and maturation of the Cvt cargo ApeI, respectively, were like the wild type in all BLOC-1 mutants (Fig. 4, B and C). We then decided to analyze endosomal integrity by localizing the Rab GTPase Vps21. Surprisingly, we observed a partial relocalization of Vps21 to the vacuole upon deletion of any BLOC-1 subunit (Fig. 4 D; unpublished data). Likewise, the Vps21 effector Vps8 moved from its exclusive dot-like localization more to the vacuole in the *kxd1Δ* mutant. This is consistent with the idea that Vps21 is not only relocalized, but also in its GTP-bound active form on vacuoles (Lachmann et al., 2012; Nickerson et al., 2012). The redistribution of Vps21 to the vacuole has been observed before in cells lacking the GAP protein Msb3 that negatively regulates Vps21 (Fig. 4 D; Lachmann et al., 2012). Of note, such a relocalization was not observed if any of the BLOC-1 subunits were C-terminally GFP tagged (Fig. 1 E), indicating that GFP tagging did not affect their functionality. Likewise, deletion of *VAC8*, the Vab2-binding partner at the vacuole, did not alter the distribution of Vps21 (Fig. S1 B).

We then hypothesized that the yeast BLOC-1 complex and Msb3 may act together and negatively regulate the endocytic flux along the endolysosomal pathway. To test this hypothesis, we decided to monitor the fate of plasma membrane (PM) transporters that are endocytosed and also recycled from the early/late endosome back to the PM (Léon et al., 2008; Lin et al., 2008; Nikko et al., 2008). One prominent example is the

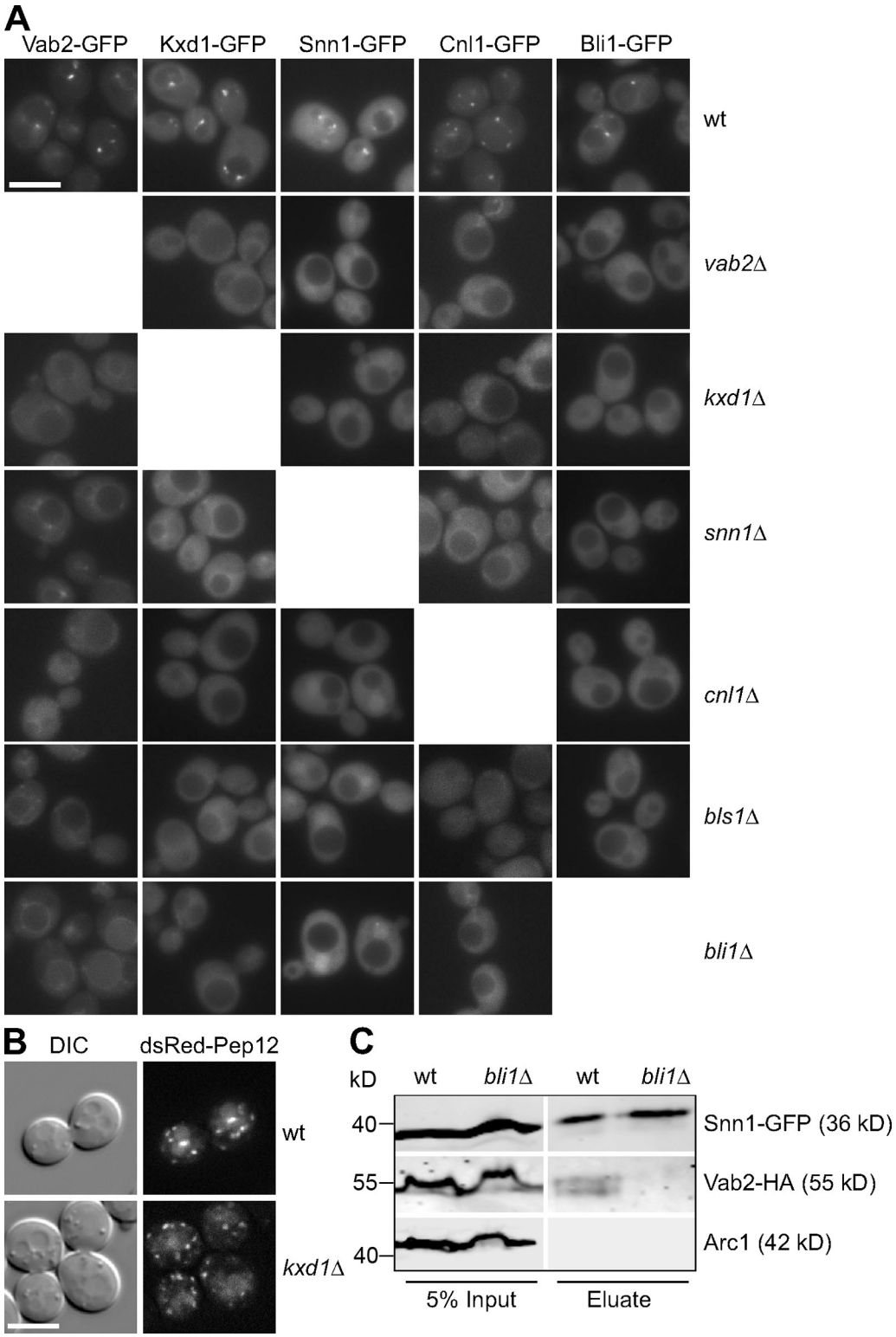

Figure 2. **Localization of BLOC-1 to endosomes requires all subunits.** (A) BLOC-1 localization depends on the intact hexameric complex. GFP-tagged subunits were localized in all respective single deletion strains and monitored by fluorescence microscopy. Bar, 5 µm. (B) Deletion of Kxd1 does not affect the localization of the endosomal SNARE Pep12. dsRed-tagged Pep12 was expressed from a CEN plasmid in wild-type and *kxd1*Δ cells and analyzed by fluorescence microscopy. Bar, 5 µm. (C) Interaction of Snn1 with Vab2. Cells expressing Snn1-GFP and Vab2-HA in wild-type (wt) and *bli1*Δ cells were subjected to immunoprecipitation via the immobilized GFP binder. Eluates from GFP beads were analyzed by SDS-PAGE and Western blotting using antibodies against HA, GFP, and Arc1 (as a control protein).

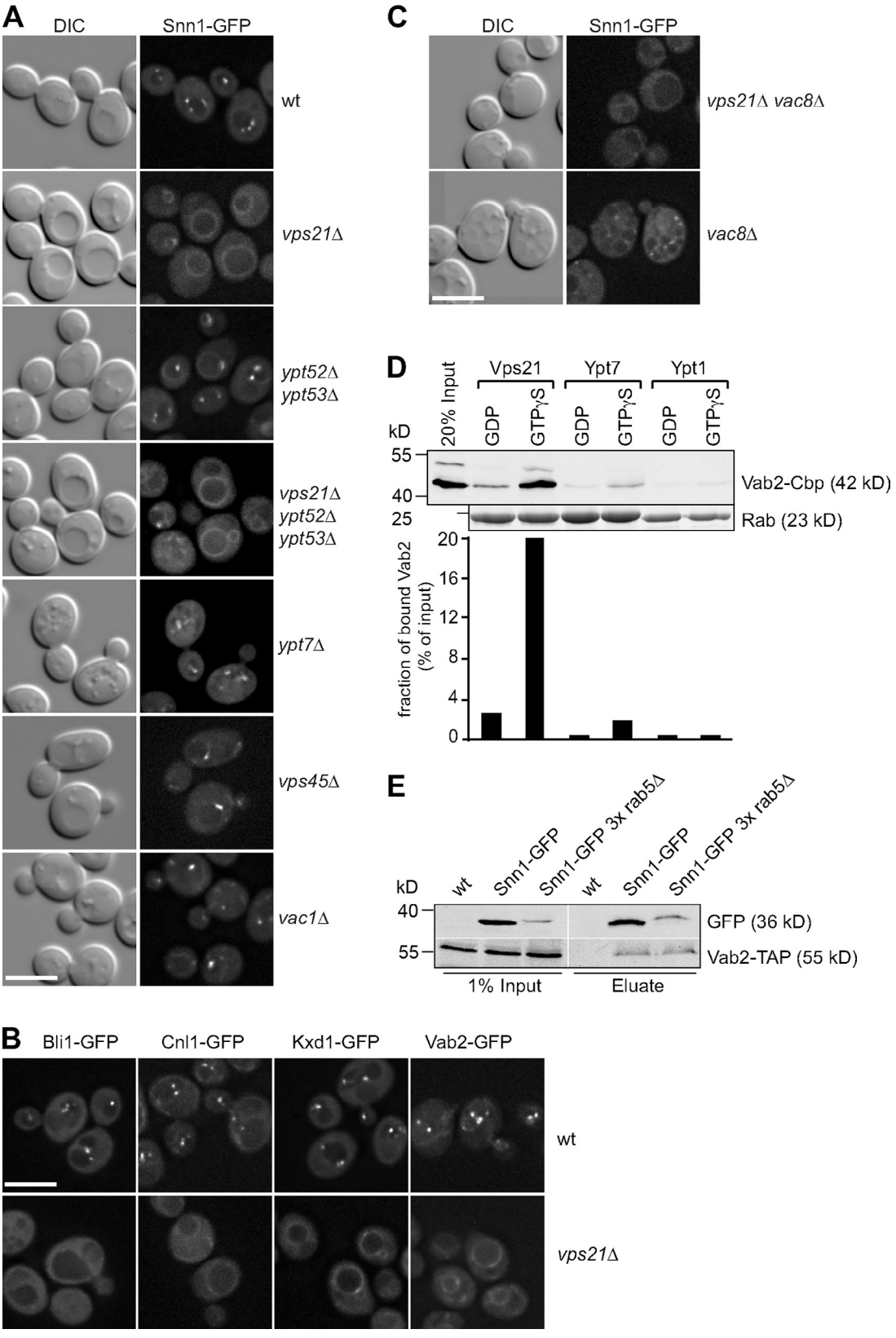

Figure 3. **BLOC-1 complex is an effector of the Rab5 homologue Vps21.** (A) Localization of BLOC-1 subunit Snn1 in the absence of Rab5 homologues and class D proteins. The respective deletion strains were analyzed by fluorescence microcopy. Depicted images were subject to 2D deconvolution. Bar, 5 µm. (B) Vps21 is required for endosomal localization of BLOC-1 subunits. The indicated BLOC-1 subunits were localized in wild-type and *vps21*Δ cells. Deconvolved images are shown. Bar, 5 µm. (C) Localization of the BLOC-1 subunit Snn1 in the absence of Vac8. The indicated strains were analyzed as in A. Bar, 5 µm. (D) Interaction of the BLOC-1 complex with Vps21. (Top) Purified BLOC-1 complex from yeast (see Materials and methods) was incubated with immobilized GST-His-Vps21, -Ypt7, and -Ypt1 that were preloaded with the indicated nucleotide. Bound proteins were eluted by high salt/EDTA,

amino acid permease Can1, which transports arginine and its toxic analogue, canavanine. Depending on the concentration of canavanine on plates, it is possible to identify mutants that affect endocytosis of Can1 or its recycling (Lin et al., 2008; Shi et al., 2011). Whereas a canavanine-sensitive phenotype typifies mutants that have excess Can1 at the PM, a canavanine-resistant phenotype implies fewer molecules of Can1 at the PM. Recently, the Ere1/2 complex was identified as a factor involved in Can1 recycling along the retromer pathway (Shi et al., 2011). Among the many canavanine-resistant mutants identified in the study were Vab2 and Msb3, suggesting that these two factors were potentially involved in Can1 recycling. We thus decided to test all BLOC-1 mutants in this assay in comparison. When we monitored the growth on canavanine plates, all BLOC-1 deletions had the same resistance phenotype compared with wild-type cells (Fig. 4 E), consistent with our observations that BLOC-1 might function as a complex. We then performed a similar assay with the toxic lysine analogue thialysine, which is a substrate of the amino acid permease Lyp1, and obtained the same resistance phenotype (Fig. 4 F). This indicates that the recycling of amino acid permease Lyp1 was also affected in BLOC-1 deletions. To test whether the resistance phenotype resulted from enhanced degradation of the receptor, we followed Can1-GFP and Lyp1-GFP by fluorescence microscopy, and found that Can1 and Lyp1 were sorted to the vacuole lumen in cells lacking the BLOC-1 protein Kxd1, even at steady state (Fig. 4, G and H). As a negative control for the sorting to vacuolar lumen, we used *vps21Δ* cells where endocytic progression is blocked. Taken together, the data indicate that the absence of BLOC-1 subunits results in an accelerated endocytic flux of the tested amino acid permeases.

We then decided to further analyze the connection between the Vps21-GAP Msb3 and the BLOC-1 complex, as these mutants resulted in a very similar phenotype (Fig. 4 D; Lachmann et al., 2012). Using the canavanine assay, we confirmed that deletion of *MSB3* also resulted in a resistant phenotype (Fig. 4 I; Shi et al., 2011) and enhanced degradation of Can1-GFP and Lyp1-GFP like that observed for BLOC-1 deletion (Fig. 4, G and H). Interestingly, a double deletion mutant *msb3Δ kxd1Δ* showed a level of resistance similar to the single deletion cells (Fig. 4 I), suggesting that they might function along the same pathway. Deletion of two other GAP proteins, Msb4 and Gyp7, which were also linked to the endocytic pathway (Brett et al., 2008), behaved like the wild type, revealing that the phenotype was Msb3 specific and not due to loss of GAP activity in general. Furthermore, the deletion of Vps21 resulted in a canavanine-sensitive phenotype that was not altered upon further deletion of either Msb3 or Kxd1. This agrees with Vps21 acting upstream of Msb3 (Lachmann et al., 2012; Nickerson et al., 2012) and BLOC-1 (shown in this paper). Furthermore, we observed that the *vac8Δ* mutant behaved as the wild type in the canavanine plate assay (Fig. S1 A), suggesting that Vac8 function is not associated with Vps21 activity.

A role for BLOC-1 in endosomal maturation

Our data suggested that Vps21, BLOC-1, and Msb3 might act in a concerted manner along the endosomal pathway. As Msb3 is the GAP protein that acts on Vps21, we hypothesized that the BLOC-1 complex might be a receptor that couples the recruitment of Msb3 to inactivation of Vps21. We would then expect that the endosomal BLOC-1 should recruit Msb3 to endolysosomal membranes. We therefore used our overexpression strain to monitor the influence of BLOC-1 on the localization of Msb3. In wild-type cells, Msb3 is found primarily on the plasma membrane, BLOC-1 in some endosomal dots, and both have a large cytosolic pool (Figs. 1 E and 5 A; Lachmann et al., 2012). Strikingly, we observed a relocalization of Msb3 to vacuoles upon induction of BLOC-1 overexpression (Fig. 5 B). Moreover, vacuoles showed a class B–like fragmentation pattern that is also observed when the function of the vacuolar Rab Ypt7 is impaired (Balderhaar et al., 2010). Indeed, BLOC-1 overexpression led to a relocalization of GFP-tagged Ypt7 to a more diffuse pattern that included ER structures. This is consistent with our previous observation that Msb3 can also act on Ypt7 (Lachmann et al., 2012). Finally, when we monitored Vps21 in the BLOC-1 overexpression strain, it was concentrated in dots at the interface between vacuoles (Fig. 5 B). In line with our observation that BLOC-1 is an effector of Vps21, a portion of the BLOC-1 subunit Bli1 localized similar to Vps21 on punctate structures between vacuoles (Fig. 5 A). We consider it likely that the excess BLOC-1 protects Vps21 from the recruited Msb3, which can, however, inactivate Ypt7 on the vacuolar membrane (Fig. 5 B). In agreement with these observations, Msb3 and the BLOC-1 subunit Vab2 could be coimmunoprecipitated, indicating that they form a complex in vivo (Fig. 5 C). We further probed the interaction between the BLOC-1 subunits and Msb3 using the split-YFP assay (Sung and Huh, 2007). In this experiment, Msb3 was N-terminally tagged with the N-terminal half of Venus (VN), a mutant version of the YFP, whereas the BLOC-1 subunits were tagged with the C-terminal half of Venus (VC). When we monitored the in vivo interaction of five of the BLOC-1 subunits, Cnl1, Snn1, and Bli1 interacted with Msb3, whereas the other two subunits, Vab2 and Bls1, did not (Fig. 5 D). Interestingly, the site of interaction was either the bud neck or exocytic sites as observed for previous interactions of Msb3 with Rabs (Lachmann et al., 2011), which is in agreement with the predominant localization of

precipitated with TCA, and analyzed by SDS-PAGE and Western blotting using anti-cbp (calmodulin-binding peptide) antibody. Rabs were eluted by boiling in SDS sample buffer. (Bottom) Percent values represent densitometric ratio of the eluted Vab2 to the amount of the respective nucleotide-loaded Rab. Quantification was performed using Quantity One software 4.6.9 (Bio-Rad Laboratories). The data represent the mean of two independent experiments. (E) Interaction of Snn1 with Vab2 in the absence of endosomal Rabs. Cells expressing Vab2-TAP alone or with Snn1-GFP in the presence or absence (*rab5Δ*) of the three endosomal Rabs (Vps21, Ypt52, Ypt53) were subjected to immunoprecipitation using the immobilized GFP binder. Note that the cellular amounts of Snn1-GFP was reduced in the absence of Rab5 GTPases. Eluates from the GFP binder beads were analyzed by SDS-PAGE, and Western blotting using antibodies against GFP and TAP tag.

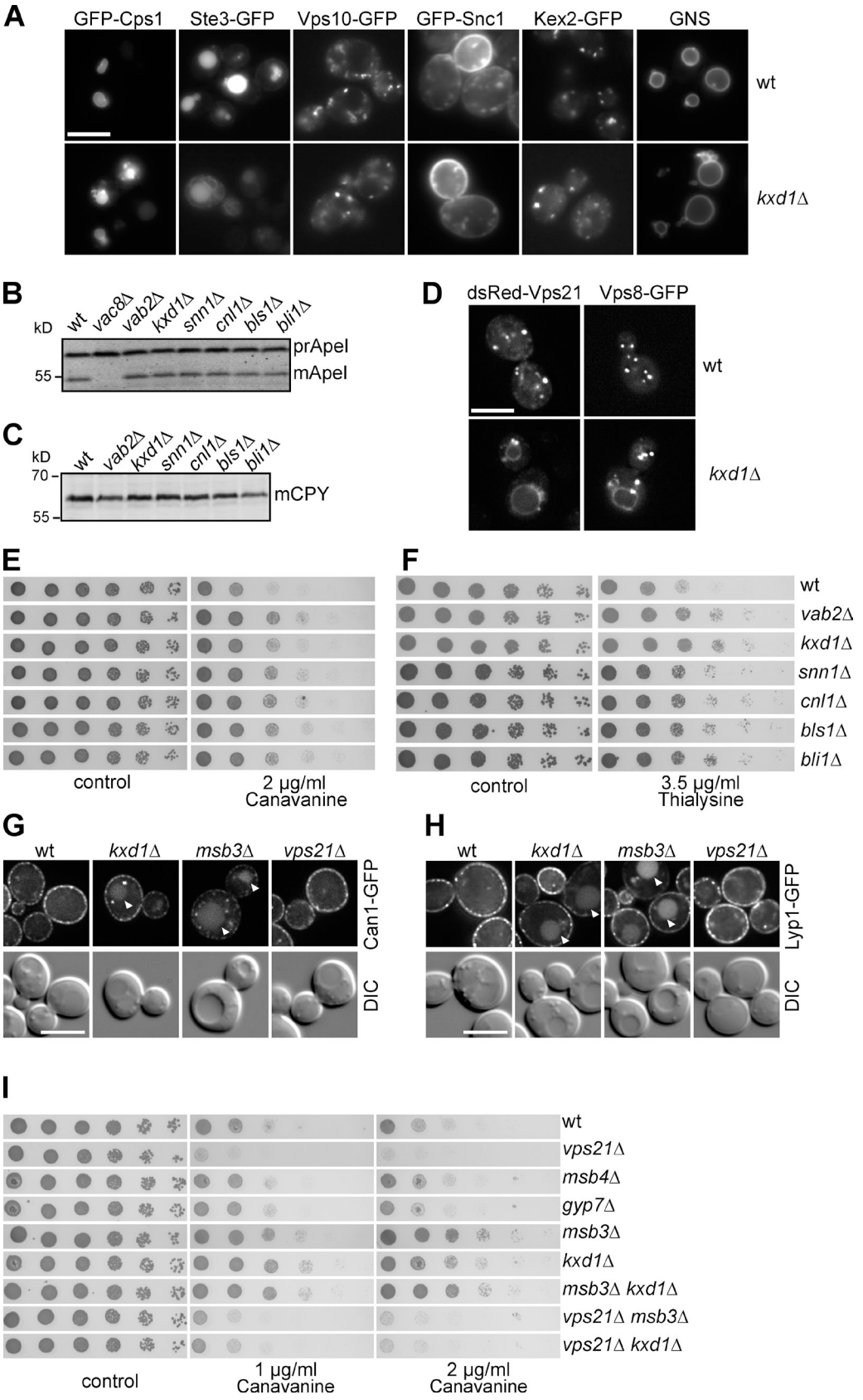

Figure 4. **Defective cargo trafficking in BLOC-1 mutants.** (A) Localization of protein-trafficking reporters. The indicated fusion proteins were localized by fluorescence microscopy in wild-type and *kxd1*Δ cells. GNS stands for GFP-Nyv1-Snc1, a reporter for the AP-3 pathway (Reggiori et al., 2000; Cabrera et al., 2010). Bar, 5 µm. (B) Sorting of Ape1 in mutant strains. Cell extracts of the indicated strains were loaded onto SDS-PAGE gels and Western blots were decorated against Ape1. *vac8*Δ served as a positive control. prApeI, precursor aminopeptidase I; mApeI, mature aminopeptidase I. (C) Sorting

endogenous Msb3 (Gao et al., 2003). Although it is likely that the observed interaction of BLOC-1 and Msb3 is independent of Vps21 and further stabilized by the interacting halves of the YFP, the data reveal that the interaction with Msb3 is mediated by specific subunits of the BLOC-1 complex.

To rule out that Msb3 recruitment was just the result of BLOC-1 overexpression and the interaction occurs only at the cell periphery, we decided to follow Msb3 recruitment to endosomes under endogenous levels of BLOC-1. As Msb3 is hardly detected on endosomes in wild-type cells, we followed its localization in the Vps21 GTP-locked mutant, reasoning that the interaction between the Rab and BLOC-1 might be prolonged. Indeed, Msb3 was now detected on dot-like structures (Fig. 6 A), which we identified as endosomes by colocalization with the endosomal Sec1–Munc18 family protein, Vps45, and the BLOC-1 subunit Kxd1 (Fig. 6, B and C). Remarkably, the endosomal localization of Msb3 was no longer observed in a BLOC-1 deletion mutant or a GDP-locked mutant of Vps21 (Fig. 6 A). Our combined data would predict that the loss of Msb3, which results in mislocalization of active Vps21 to the vacuole surface, would also affect BLOC-1 localization. Indeed, we observed a significant relocalization of Kxd1-GFP to vacuoles upon loss of Msb3 or when Vps21 was in the dominant-active form (Fig. 6 D).

Overproduction of GAPs has been taken as one criterion to determine their specificity in vivo (Brett et al., 2008). We thus wondered if excess Msb3 might bypass the need of BLOC-1 as a receptor, and thus overexpressed Msb3 from the strong *GAL1* promoter. In glucose-containing medium, Msb3 is not expressed and Vps21 is found on vacuoles as previously shown (Lachmann et al., 2012; Nickerson et al., 2012). Upon overproduction, we then observed mislocalization of Vps21 even in the absence of the BLOC-1 subunit Kxd1 (Fig. 6 E), indicating that GAP overproduction might bypass any regulator or receptor such as BLOC-1.

In summary, our data strongly indicate that BLOC-1 is a Vps21 effector as well as a negative regulator, which recruits the GAP Msb3 and thus controls the Vps21 nucleotide cycle and endosome maturation (Fig. 6 F).

Discussion

Our data reveal that the BLOC-1 complex is an evolutionarily conserved endosomal protein complex, which is involved in receptor trafficking and endosomal maturation. BLOC-1 consists of six subunits and requires all of its subunits and the Rab5 GTPase Vps21 for endosomal recruitment (Figs. 2 and 3). In fact, we find that BLOC-1 is a Vps21 effector, which is further supported by a loss of endosomal localization in the absence of Vps21. Our data uncover BLOC-1 as the receptor of the Rab5/Vps21-GAP Msb3, which in turn regulates Rab activity on endosomes (Fig. 6 F). Several findings support this model. First, *msb3* and BLOC-1 mutants have similar phenotypes on Vps21 localization and permease trafficking (Fig. 4) (Lachmann et al., 2012; Nickerson et al., 2012). Msb3 relocalizes to the vacuolar surface upon overexpression of the entire BLOC-1 complex, which also shifts Vps21 to the interface between vacuoles (Fig. 5 B). Furthermore, Msb3 requires BLOC-1 and Vps21-GTP to localize to endosomes (Fig. 6 A). Finally, in the absence of Msb3, BLOC-1 is found on vacuoles like Vps21 (Fig. 6 D), in agreement with a function of Msb3 in the same pathway, but downstream of Vps21 and BLOC-1. Our combined data show that BLOC-1 is an adapter that couples Rab activity to its GAP, and provides an unexpected paradigm in the context of endosomal maturation.

A function of BLOC-1 at the endosome has been predicted for the metazoan BLOC-1 based on its localization to tubular endosomes (Di Pietro et al., 2006). Likewise, BLOC-1 has been correlated to Rab11-function, though neither direct interaction nor function of the interaction could be shown, presumably due to overlapping activities of metazoan Rabs (Rodriguez-Fernandez and Dell'Angelica, 2009). Taking into account that the metazoan BLOC-1 has at least eight subunits, and an elongated structure (Lee et al., 2012), multiple interaction sites on membranes are expected. In yeast, we found that the localization of BLOC-1 to endosomes is strongly dependent on Vps21, whereas the redistribution to vacuoles in *vps21Δ* cells is dictated by Vac8 (Fig. 3, A–C). Loss of Vac8 does not affect the punctate localization of the BLOC-1 subunit Snn1-GFP, indicating that Vac8 does not play a major role in BLOC-1 recruitment to endosomes. We can, however, not exclude that Vac8, which binds Vab2 in vivo (Fig. 5 C; Pan et al., 2000), also affects the availability of Vab2 for the BLOC-1 complex. This is an issue for future investigations.

Defects in BLOC-1 are tightly linked to the missorting of TYRP1 and AP-3 cargo such as LAMP1 away from lysosome-related organelles and lysosomes, respectively (Di Pietro et al., 2006; Salazar et al., 2006, 2009). For the yeast BLOC-1, it is the central endosomal pathway that is affected. Deletions of either *BLOC-1* or *MSB3* genes result in cells with less Can1 and Lyp1 permeases on their surface, which are presumably sorted to the vacuole lumen before they can be recycled (Fig. 4, G and H). Taking into account that these mutants carry hyperactive Vps21, we consider it likely that the resulting increase in endosomal fusion events might overwhelm the functional capacity of the recycling machinery, and thus drive the permeases to the vacuole for degradation. However, it is important to keep in mind

of CPY in BLOC-1 mutants. Cell extracts were prepared as before and decorated against CPY. mCPY, mature carboxypeptidase Y. (D) Vps21 and its effector Vps8 are relocated to the vacuole in the *kxd1Δ* mutant. dsRed-tagged Vps21 and GFP-tagged Vps8 were localized by fluorescence microscopy. Deconvolved images are shown. Bar, 5 µm. (E) BLOC-1 mutant strains are canavanine resistant. Wild-type and BLOC-1 mutants were spotted as serial dilutions onto synthetic media plates without or with 2 µg/ml canavanine. Plates were photographed after two days of growth. For details, see Materials and methods. (F) BLOC-1 mutant strains are thialysine resistant. Wild-type and BLOC-1 mutants were spotted as serial dilutions onto synthetic media plates without or with 3.5 µg/ml thialysine. Plates were photographed after two days of growth. For details, see Materials and methods. (G) Localization of Can1-GFP in *kxd1Δ* and *msb3Δ* cells. Early log phase cells expressing Can1-GFP were examined by fluorescence microscopy. Deconvolved images are shown. Arrowheads indicate Can1-GFP in the vacuole lumen. Bar, 5 µm. (H) Localization of Lyp1-GFP in *kxd1Δ* and *msb3Δ* cells. Early log phase cells expressing Lyp1-GFP were examined by fluorescence microscopy. Deconvolved images are shown. Arrowheads indicate Lyp1-GFP in the vacuole lumen. Bar, 5 µm. (I) BLOC-1 and Msb3 act along the same pathway. The indicated mutant strains were checked for canavanine resistance as described before.

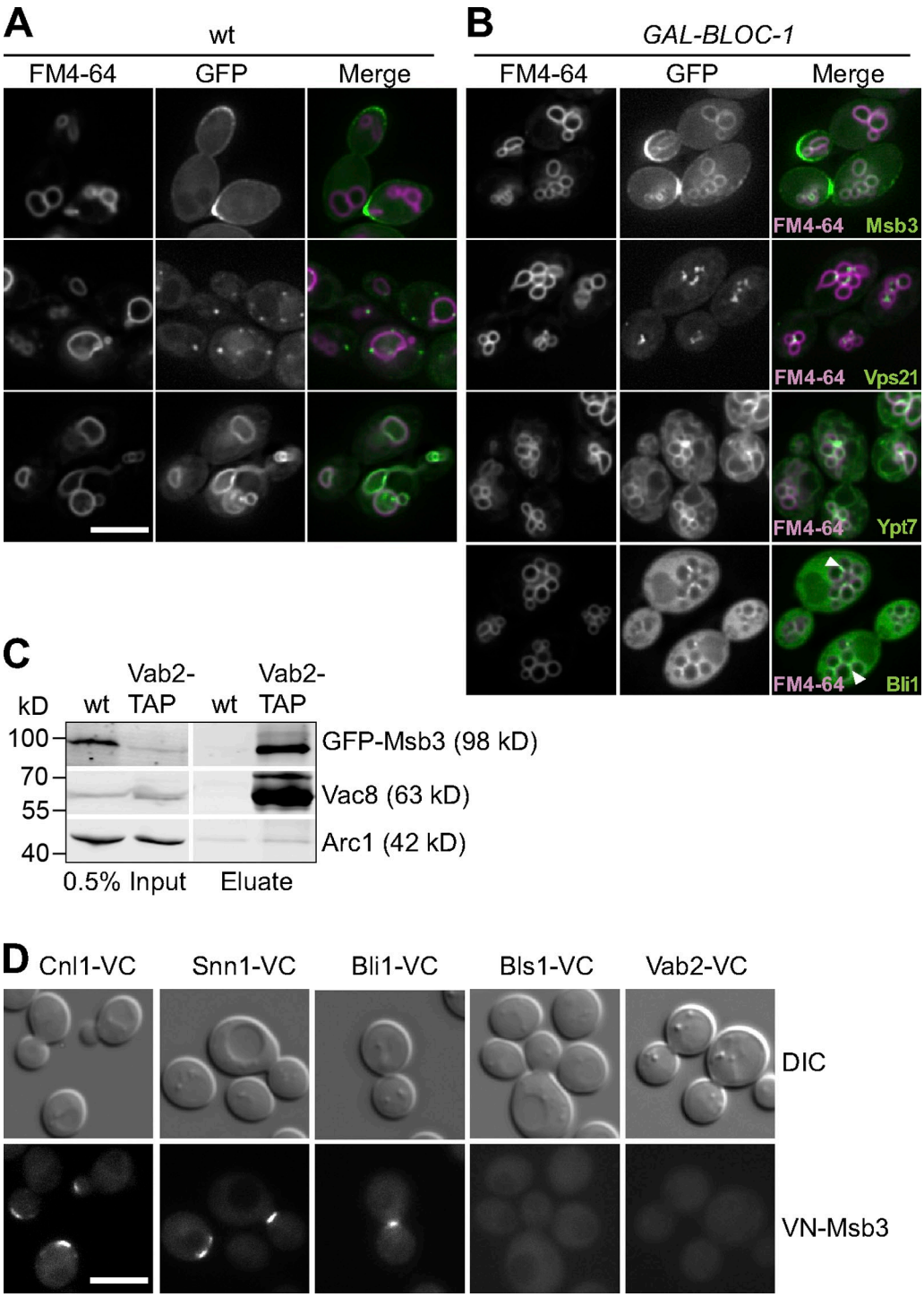

Figure 5. **BLOC-1 is a receptor for Msb3.** (A and B) BLOC-1 overproduction relocalizes Msb3 to the vacuole surface. GFP-tagged Msb3, Ypt7, and Vps21 were localized by fluorescence microscopy in diploid wild-type cells or cells overexpressing the entire BLOC-1 under the control of the *GAL1* promoter. Bli1-GFP was monitored only in the BLOC-1 overexpression strain. To monitor vacuole morphology, membranes were stained with FM4-64. Deconvolved images are shown. Arrowheads indicate Bli1-GFP accumulation at the vacuole–vacuole interface. Bar, 5 µm. (C) Msb3 interacts with BLOC-1. Cell lysates containing GFP-tagged Msb3 alone or with overproduced BLOC-1 complex were immunoprecipitated with IgG Sepharose. Eluates were TCA precipitated and analyzed by SDS-PAGE and Western blotting using antibodies against GFP, Vac8, and Arc1 (as a control protein). (D) BLOC-1 subunits Cnl1, Snn1, and Bli1 interact with Msb3 in vivo. VN-Msb3 and BLOC1-VC were coexpressed, and the interaction was visualized by the YFP signal. Bar, 5 µm.

that a canavanine-resistant phenotype or elevated Can1 degradation might also result from a defect in recycling as has been demonstrated for retromer and *snx* mutants (Shi et al., 2011). Therefore, it remains to be seen whether the effect of BLOC-1 on the recycling of the two permeases is direct or indirect.

One central issue of this work is the identification of BLOC-1 as an adapter between a Rab and its own GAP. This raises several issues. First, our data provide evidence that GAPs rely on binding partners to act at the right position and time. For instance, the localization of Msb3 to the polarized growth sites

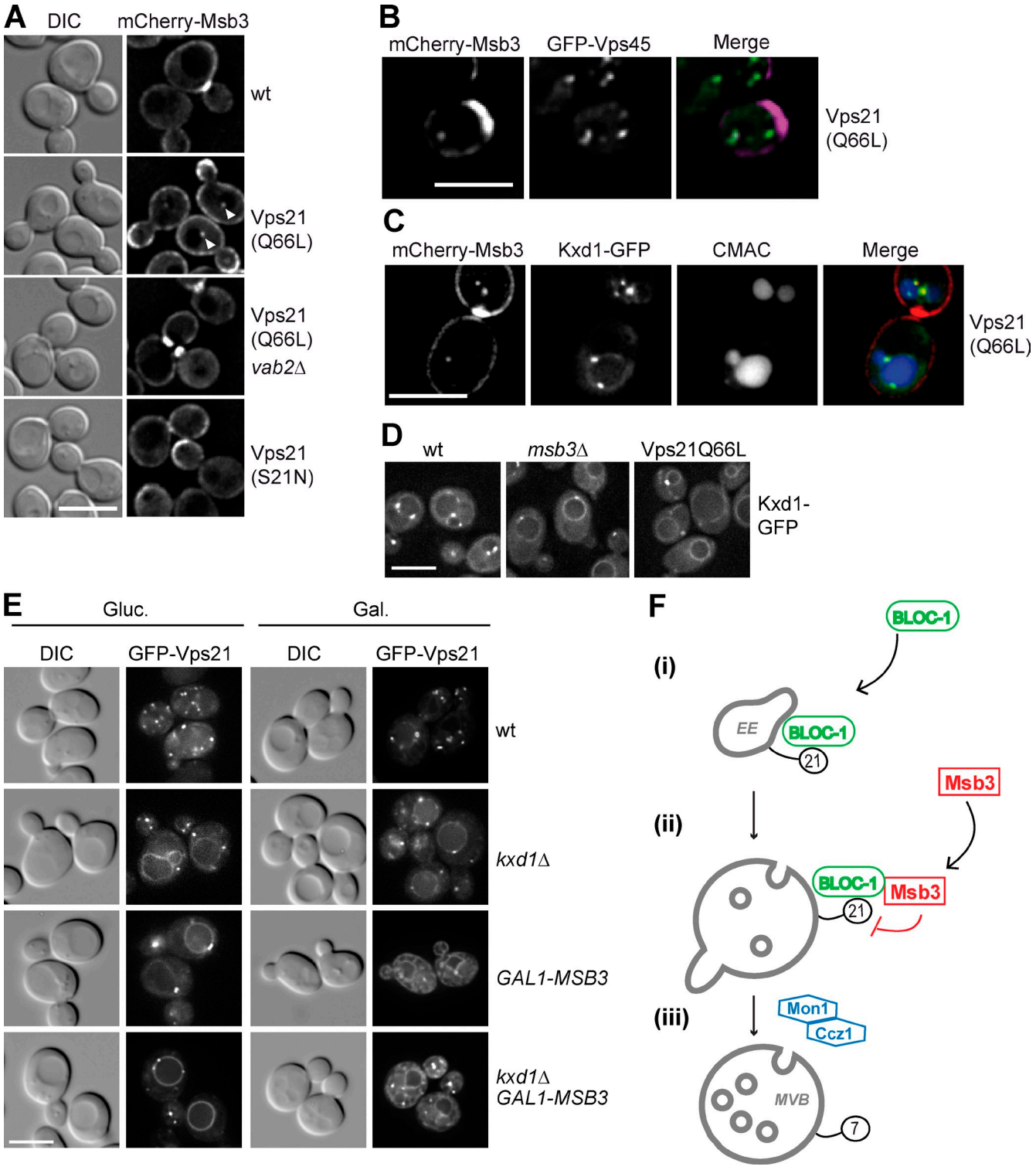

Figure 6. **Msb3 recruitment to endosomes is dependent on BLOC-1.** (A) Msb3 localizes to endosomes in the Vps21 (Q66L) mutant. mCherry-tagged Msb3 was localized in the indicated strains. Images were subjected to 3D deconvolution and a single slice from a Z-stack is depicted. Arrowheads indicate the endosomal dot-like structures. Bar, 5 µm. (B) Msb3 colocalizes with Vps45 in the Vps21 (Q66L) mutant. Localization of mCherry-tagged Msb3 and GFP-tagged Vps45 was examined as in A. Bar, 5 µm. (C) Msb3 colocalizes with Kxd1 in the Vps21 (Q66L) mutant. Localization of mCherry-tagged Msb3 and GFP-tagged Kxd1 is depicted as a sum projection of three Z-slices, after 3D deconvolution, to clearly visualize the colocalizing endosomal population and the vacuolar localization of Kxd1 in the Vps21 GTP-locked mutant. CMAC staining of vacuoles is also shown. Bar, 5 µm. (D) Kxd1 mislocalization upon hyperactivation of Vps21. GFP-tagged Kxd1 was localized in wild-type, *msb3Δ*, and Vps21 (Q66L) mutants and analyzed by fluorescence microscopy. Depicted images were subjected to 2D deconvolution. Bar, 5 µm. (E) Excess of Msb3 can displace Vps21 from membranes in the absence of BLOC-1. GFP-Vps21 was monitored in strains carrying *MSB3* gene under the control of the *GAL1*-promoter. Cells were grown in glucose (Gluc.) or galactose (Gal.) and then analyzed as in D. Bar, 5 µm. (F) Model of BLOC-1 function in the endocytic pathway. BLOC-1 requires active Vps21 for endosome association (i). On endosomes, BLOC-1 recruits Msb3 to membranes, which results in Vps21 inactivation (ii). The Mon1–Ccz1 GEF complex is then required to activate Ypt7 on late endosomes (iii).

is Cdc42 dependent (Bi et al., 2000), but its receptor at the plasma membrane has not been identified. Likewise, the putative Rab7 GAP, TBC1D5, interacts with the Vps retromer subcomplex at endosomes and Atg8 at autophagosomes (Seaman et al., 2009; Popovic et al., 2012), though its precise function remains unexplored. Rabs can thus recruit their own GAP via an adapter as shown here for BLOC-1. Potentially, the association of Msb3 with BLOC-1 restricts its activity on endosomes to avoid premature Rab inactivation. This would explain why overexpressed Msb3 is able to displace Vps21 from endosomes, even if BLOC-1 is deleted (Fig. 6 E). BLOC-1 may thus be the first example of a GAP adapter in the context of Rab GTPases, and could explain how GAPs like Msb3 can act at multiple locations by using bridging adapters and control the timing of their inactivation (Gao et al., 2003). It is notable that a similar module exists for the Arf1 GTPase, where its effector, the COPI coat, recruits the Arf1GAP to inactivate the GTPase and regulate its disassembly (Liu et al., 2005).

Second, our findings leave the question open, how the nucleotide cycles of distinct Rabs are coordinated. Previously, at least two studies reported a negative feedback loop, which can facilitate the Rab exchange process (Hutagalung and Novick, 2011). For Gyp1, which inactivates Rab1/Ypt1 at the Golgi, the downstream Rab Ypt31 was identified as the apparent GAP receptor (Rivera-Molina and Novick, 2009). Likewise, for the Rab5 to Rab7 conversion in *Caenorhabditis elegans*, it was proposed that Rab7 recruits the GAP TBC-2 for the upstream GTPase Rab5 (Chotard et al., 2010). Whereas Ypt32 and Gyp1 can interact directly, the link between Rab7 and TBC-2 remains indirect. However, it is striking that *C. elegans* TBC-2 can also act on Rab7, similar to Msb3, which acts on Ypt7 as well (Chotard et al., 2010; Lachmann et al., 2012; Nickerson et al., 2012). Potentially, Rab7 takes advantage of adapters to control the GAP activity of TBC-2.

Third, we do not yet understand the sequence of events responsible for the Rab exchange during endosomal maturation. In this context, if we assume that Ypt7 is only recruited to mature endosomes upon inactivation and subsequent release of Vps21, then the Ypt7 GEF Mon1–Ccz1 complex might be required to coordinate the function of BLOC-1/Msb3 with Ypt7 recruitment and activation (Fig. 6 F).

In summary, our data provide evidence for BLOC-1 as a novel GAP regulator complex that binds to both Rab and the cognate GAP protein. Furthermore, we can now start to understand BLOC-1 function in metazoan cells, which is likely to use a similar mechanism to localize to endosomes—potentially via Rab11—and inactivate the same Rab. We consider this an important step forward also to understand the function of BLOC-2 and BLOC-3 complexes, the latter being a Rab9 and Rab32/38 GEF effector (Kloer et al., 2010; Gerondopoulos et al., 2012), and thus the defects associated with Hermansky-Pudlak syndrome.

Materials and methods

Yeast strains and molecular biology

Strains used in this study are listed in Table S1. N-terminal tagging, C-terminal tagging, and deletion of genes were done using homologous recombination of PCR fragments (Puig et al., 1998; Janke et al., 2004). Deletion of genes was confirmed by colony PCR using a forward primer that annealed to the upstream region of the respective gene and a reverse primer that annealed to the marker gene used for deletion.

Plasmids

GFP-Nyv1-Snc1 fusion gene cloned into the pRS416 plasmid expressed from the TPI promoter (pGNS) was provided by F. Reggiori (UMC Utrecht, Utrecht, Netherlands). dsRed-tagged Vps21 and Pep12 cloned into the pRS411 plasmid was expressed from the PHO5 promoter. These constructs were derived from the plasmid pV2-dsRed provided by A. Gillingham (MRC-LMB, Cambridge, England, UK). GFP-Cps1 cloned into the pRS426 plasmid was provided by M. Babst (Univerity of Utah, Salt Lake City, UT). Can1-GFP cloned into the pRS416 plasmid was provided by S. Emr (Cornell University, Ithaca, NY). To check Can1-GFP localization expressed from a CEN plasmid, cells were grown in SDC medium lacking uracil. For localization of the genomically GFP-tagged Lyp1, cells harbored a pRS317 plasmid to complement lysine auxotrophy and were grown in SDC medium lacking lysine.

For split-YFP, the tested BLOC-1 subunits were amplified from genomic DNA, digested with BamHI and SmaI and inserted into BamHI–SmaI sites of pME3406 that harbors the C-terminal half of YFP (155–238) under the control of the MET25 promoter. The backbone plasmid was kindly provided by G. Braus (University of Göttingen, Göttingen, Germany).

Microscopy

Yeast cells were grown to mid-log phase in YPD or YPG collected by centrifugation, washed once with SDC or SGC medium supplemented with all amino acids, spotted on the glass, and analyzed by fluorescence microscopy. For FM4-64 staining of vacuoles, cells were incubated with 30 µM FM4-64 for 20 min, washed twice with YPD medium, and incubated in the same medium without dye for 1 h at 30°C. For the split-YFP assay, *MSB3* was genomically tagged with the N-terminal half of YFP and expression was driven by the CET1 promoter. BLOC-1 subunits were C-terminally tagged with YFP and expressed from a *CEN* plasmid. To maintain plasmids and for inducing expression of MET25 promoter, cells were grown in synthetic medium lacking selected amino acids to mid-log phase before analysis. Microscopy was performed at room temperature. Images were acquired with a microscope (DM5500 B; Leica) equipped with an HCX PL-APO 100× (1.46 NA) oil immersion objective, a SPOT Pursuit camera (Leica), filter sets for DIC, GFP, RFP, and FM4-64 (Chroma Technology Corp.), and MetaMorph 7 software (Visitron Systems). Images were processed using Adobe Photoshop CS3 and assembled on Adobe Illustrator CS3. Where indicated, images were subjected to 2D deconvolution using Auto Quant X software (Media Cybernetics). For some experiments, images were acquired on an imaging system (Deltavision Elite; GE Healthcare) based on an inverted microscope (model IX-71; Olympus), equipped with an UAPON 100× (1.49 NA) oil immersion objective, an InsightSSI light source (Applied Precision), excitation and emission filters for DAPI, FITC, TRITC, and a CoolSNAP HQ^2 CCD camera (Photometrics). Stacks of 8 or 10 images with 0.2-µm spacing were subjected to 3D deconvolution using SoftWoRx 5.5 software (Applied Precision). Processing of the images was performed with ImageJ 1.42q (National Institutes of Health) and Adobe Photoshop CS4.

Yeast cell lysis

For monitoring endogenous expression of C-terminally GFP-tagged BLOC-1 subunits, 1 OD_{600} of mid-log phase cells were collected by centrifugation and were precipitated using 10% trichloroacetic acid for 20 min at 4°C. After centrifugation at 13,000 *g* for 5 min, pellets were washed with ice-cold acetone. Pellets were air-dried and resuspended in 30 µl of 1× SDS sample buffer (60 mM Tris, pH 6.8, 2% SDS, 10% glycerol, 5% 2-mercaptoethanol, and 0.005% bromophenol blue), and boiled for 3 min. Samples were resolved on a 12% SDS-PAGE gel, and after Western transfer, proteins were detected using anti-GFP antibody (Roche).

Canavanine and thialysine growth assay

Cells were grown to mid-log phase in YPD medium, washed once with SDC medium supplemented with all amino acids except arginine, and spotted onto SDC-arginine agar plates containing the indicated concentration of canavanine. For the thialysine assay, cells were grown in SDC medium supplemented with all amino acids except lysine, and spotted onto SDC-lysine agar plates containing the indicated concentration of thialysine. Plates were incubated at 26°C for 2 d. For spotting, serial (fourfold) dilutions were made with the first spot in each row corresponding to 0.25 OD_{600}.

Rab purification and Rab pull-down

His-GST-Rab expression constructs (Bröcker et al., 2012; Lachmann et al., 2012) were transformed into Rosetta *Escherichia coli* strains, and protein

production was induced with IPTG overnight at 18°C. Pelleted bacteria were lysed in a lysis buffer containing 20 mM Tris, pH 8.0, 150 mM NaCl, 5 mM imidazole, 1 mM PMSF, and protease inhibitor cocktail (Roche). Lysates were cleared by centrifugation at 20,000 *g* for 15 min at 4°C. Supernatants containing His-GST fusion proteins were incubated with Ni-NTA agarose beads (QIAGEN) for 2 h at 4°C. Beads were washed extensively in lysis buffer, and eluted with the same buffer containing 200 mM imidazole. Eluates containing the purified Rab protein were then applied and eluted from a PD10 column (GE Healthcare) that was equilibrated in 20 mM Hepes-NaOH, pH 7.4, 100 mM NaCl, and 1 mM $MgCl_2$.

Purified His-GST-Rabs were charged with GDP or GTP-γs in a buffer containing 200 mM Hepes-NaOH, pH 7.4, 20 mM EDTA, and 25 mM $MgCl_2$ by incubation at 30°C for 15 min. The nucleotide-loaded Rabs were bound to 50 µl of prewashed GSH beads at 4°C for 1 h. Subsequently, BLOC-1 complex purified from the overexpression strain was incubated with the respective GDP/GTP-γs-loaded Rab for 1 h at 4°C. The beads were washed twice with 20 mM Hepes-NaOH, pH 7.4, 100 mM NaCl, 1 mM $MgCl_2$, and 0.1% Triton X-100. The bound BLOC-1 complex was eluted with 20 mM Hepes-NaOH, pH 7.4, 200 mM NaCl, 20 mM EDTA, and 0.1% Triton X-100, TCA precipitated, and analyzed by SDS-PAGE and Western blotting using anti-TAP antibody, which recognizes the TAP-tagged BLOC-1 subunit Vab2. The GSH beads were boiled in 1× SDS sample buffer, and the eluates were loaded onto SDS-PAGE gels to monitor the amount of the Rab proteins bound to GSH beads.

Purification of GFP-binding protein and coupling to NHS-activated Sepharose

The 13-kD His-tagged GFP-binding protein (GFP binder) was purified using Ni-NTA beads as described for the purification of Rabs. Imidazole-eluted fractions were pooled and the buffer was exchanged to coupling buffer (0.2 M $NaHCO_3$ and 0.5 M NaCl, pH 8.45). For coupling of the GFP binder to NHS-activated Sepharose, the reaction was performed according to the manufacturer's instructions (GE Healthcare). In brief, 1.5 mg of the purified GFP-binding protein was incubated with 1 ml NHS-activated Sepharose for 2 h at 4°C. After coupling, nonreacted groups were blocked by incubating the medium with 0.5 M ethanolamine and 0.5 M NaCl, pH 8.3. The medium was washed with 0.1 M Tris-HCl, pH 8.5, and 0.1 M acetic acid, 0.5 M NaCl, pH 4.5 alternatively for three times. The GFP binder beads were stored at 4°C in 50 mM Tris, pH 7.4, and 150 mM NaCl containing 0.02% sodium azide until further use.

GFP pull-down

250 OD units of mid-log phase cells grown overnight in YPD were washed in cold PBS and resuspended in 300 µl TE buffer (50 mM Tris, pH 7.5, 1 mM EDTA, 1× PIC, 0.5 mM PMSF, and 0.5% NP-40). Glass beads were added and cells were lysed using a Disrupter Genie (Scientific Industries, Inc.). The lysate was centrifuged at 20,000 *g* for 10 min and the supernatant was further centrifuged at 100,000 *g* for 30 min. The supernatant was precleared by incubation with 25 µl of Sepharose beads, prewashed with TE buffer for 1 h at 4°C on a turning wheel. After centrifugation, the precleared lysate was incubated with 25 µl of GFP binder beads overnight at 4°C on a turning wheel. After washing the beads with TN buffer (10 mM Tris, pH 7.5, 500 mM NaCl, and 1× PIC), the bound proteins were eluted with 100 µl 4× SDS sample buffer and subsequent boiling for 5 min at 95°C.

Tandem affinity purification (TAP)

One liter culture of wild-type and BLOC-1 overexpression (with a TAP-tagged Vab2) strains grown to an OD_{600} of 8 in YPG medium were harvested and washed once in distilled water. The pellet was resuspended in lysis buffer (20 mM Hepes, pH 7.4, 300 mM NaCl, 1 mM $MgCl_2$, 0.1% NP-40, 5% glycerol, 1 mM PMSF, and protease inhibitor cocktail) and an equal volume of glass beads was added for disruption of cells using a Planetary Mono Mill Pulverisette 6 (Fritsch). The lysate was centrifuged at 3,000 *g* for 10 min. The resulting supernatant was further centrifuged at 100,000 *g* for 1 h. Subsequently, the clear supernatant was incubated with Sepharose 6 beads (GE Healthcare) at 4°C for 1 h. The Sepharose beads were pelleted, and the supernatant was incubated with IgG beads at 4°C for 2 h. After centrifugation, the IgG beads were washed twice with lysis buffer containing 0.5% NP-40. The bound proteins were eluted with 0.1 M glycine, pH 2.5, TCA precipitated, solubilized in 1× SDS sample buffer, and loaded on a 4–20% SDS polyacrylamide gradient gel. The protein bands were visualized by colloidal Coomassie staining. For gel filtration and phospholipid-binding experiments, BLOC-1 complex was eluted with a TEV (tobacco etch virus) protease that recognizes and cleaves at the TEV cleavage site, separating the calmodulin-binding peptide and the protein A sequence in the TAP tag.

Gel filtration

Purified BLOC-1 complex as described above was loaded onto a Superose 12 10/300 GL column (GE Healthcare) connected to an ÄKTA-FPLC-system (GE Healthcare), and equilibrated with 20 mM Hepes-NaOH, pH 7.4, 300 mM NaCl, 5% glycerol, 1 mM $MgCl_2$, and 0.1% NP-40. The flow rate was set to 0.5 ml/min and 24 one-ml fractions were collected. For analysis, the fractions were TCA precipitated and loaded onto a 4–12% SDS-PAGE gradient gel (NuPAGE; Invitrogen).

Online supplemental material

Fig. S1 shows the canavanine assay (A) and GFP-Vps21 localization (B) for wild-type and *vac8Δ* cells. Table S1 lists the yeast strains used in the study. Online supplemental material is available at http://www.jcb.org/cgi/content/full/jcb.201210038/DC1.

We would like to thank S. Engelbrecht-Vandré for the structure analysis of BLOC-1; S. León for sharing reagents; A. Gillingham, F. Reggiori, G. Braus, and S. Emr for sharing plasmids; T. Levine, M. Babst, and J. MacGurn for insightful discussions; M. Schuldiner and G. Cohen for the GFP-binder plasmid and related discussions; E. Hurt for providing the Arc1 antibody; S. Walter for protein identification by Mass Spectrometry; and members of the Ungermann laboratory for critical suggestions.

This work was supported by the University of Osnabrück graduate program, the DAAD program, the Boehringer Ingelheim Fonds, the SFB 944 graduate program, and the Lichtenberg stipends of the State of Lower Saxony (to A.T. John Peter), the SFB 944 (project P11), and by the Hans-Mühlenhoff foundation (to C. Ungermann).

Submitted: 8 October 2012
Accepted: 1 March 2013

References

Babu, M., J. Vlasblom, S. Pu, X. Guo, C. Graham, B.D.M. Bean, H.E. Burston, F.J. Vizeacoumar, J. Snider, S. Phanse, et al. 2012. Interaction landscape of membrane-protein complexes in *Saccharomyces cerevisiae*. *Nature*. 489:585–589. http://dx.doi.org/10.1038/nature11354

Balderhaar, H.J.K., H. Arlt, C.W. Ostrowicz, C. Bröcker, F. Sündermann, R. Brandt, M. Babst, and C. Ungermann. 2010. The Rab GTPase Ypt7 is linked to retromer-mediated receptor recycling and fusion at the yeast late endosome. *J. Cell Sci.* 123:4085–4094. http://dx.doi.org/10.1242/jcs.071977

Bi, E., J.B. Chiavetta, H. Chen, G.C. Chen, C.S. Chan, and J.R. Pringle. 2000. Identification of novel, evolutionarily conserved Cdc42p-interacting proteins and of redundant pathways linking Cdc24p and Cdc42p to actin polarization in yeast. *Mol. Biol. Cell*. 11:773–793.

Bonifacino, J.S., and J.H. Hurley. 2008. Retromer. *Curr. Opin. Cell Biol.* 20:427–436. http://dx.doi.org/10.1016/j.ceb.2008.03.009

Brett, C.L., R.L. Plemel, B.T. Lobingier, M. Vignali, S. Fields, A.J. Merz, and A.J. Merz. 2008. Efficient termination of vacuolar Rab GTPase signaling requires coordinated action by a GAP and a protein kinase. *J. Cell Biol.* 182:1141–1151. http://dx.doi.org/10.1083/jcb.200801001

Bröcker, C., A. Kuhlee, C. Gatsogiannis, H.J. Balderhaar, C. Hönscher, S. Engelbrecht-Vandré, C. Ungermann, and S. Raunser. 2012. Molecular architecture of the multisubunit homotypic fusion and vacuole protein sorting (HOPS) tethering complex. *Proc. Natl. Acad. Sci. USA*. 109:1991–1996. http://dx.doi.org/10.1073/pnas.1117797109

Cabrera, M., L. Langemeyer, M. Mari, R. Rethmeier, I. Orban, A. Perz, C. Bröcker, J. Griffith, D. Klose, H.-J. Steinhoff, et al. 2010. Phosphorylation of a membrane curvature-sensing motif switches function of the HOPS subunit Vps41 in membrane tethering. *J. Cell Biol.* 191:845–859. http://dx.doi.org/10.1083/jcb.201004092

Cabrera, M., H. Arlt, N. Epp, J. Lachmann, J. Griffith, A. Perz, F. Reggiori, and C. Ungermann. 2012. Functional separation of endosomal fusion factors and the corvet tethering complex in endosome biogenesis. *J. Biol. Chem.* 288:5166–5175. http://dx.doi.org/10.1074/jbc.M112.431536

Cheli, V.T., R.W. Daniels, R. Godoy, D.J. Hoyle, V. Kandachar, M. Starcevic, J.A. Martinez-Agosto, S. Poole, A. DiAntonio, V.K. Lloyd, et al. 2010. Genetic modifiers of abnormal organelle biogenesis in a *Drosophila* model of BLOC-1 deficiency. *Hum. Mol. Genet.* 19:861–878. http://dx.doi.org/10.1093/hmg/ddp555

Chotard, L., A.K. Mishra, M.A. Sylvain, S. Tuck, D.G. Lambright, and C.E. Rocheleau. 2010. TBC-2 regulates RAB-5/RAB-7-mediated endosomal trafficking in Caenorhabditis elegans. *Mol. Biol. Cell*. 21:2285–2296. http://dx.doi.org/10.1091/mbc.E09-11-0947

Cullen, P.J. 2008. Endosomal sorting and signalling: an emerging role for sorting nexins. *Nat. Rev. Mol. Cell Biol.* 9:574–582. http://dx.doi.org/10.1038/nrm2427

Dell'Angelica, E.C. 2004. The building BLOC(k)s of lysosomes and related organelles. *Curr. Opin. Cell Biol.* 16:458–464. http://dx.doi.org/10.1016/j.ceb.2004.05.001

Dell'Angelica, E.C. 2009. AP-3-dependent trafficking and disease: the first decade. *Curr. Opin. Cell Biol.* 21:552–559. http://dx.doi.org/10.1016/j.ceb.2009.04.014

Di Pietro, S.M., J.M. Falcón-Pérez, and E.C. Dell'Angelica. 2004. Characterization of BLOC-2, a complex containing the Hermansky-Pudlak syndrome proteins HPS3, HPS5 and HPS6. *Traffic*. 5:276–283. http://dx.doi.org/10.1111/j.1600-0854.2004.0171.x

Di Pietro, S.M., J.M. Falcón-Pérez, D. Tenza, S.R.G. Setty, M.S. Marks, G. Raposo, and E.C. Dell'Angelica. 2006. BLOC-1 interacts with BLOC-2 and the AP-3 complex to facilitate protein trafficking on endosomes. *Mol. Biol. Cell*. 17:4027–4038. http://dx.doi.org/10.1091/mbc.E06-05-0379

Gao, X.-D., S. Albert, S.E. Tcheperegine, C.G. Burd, D. Gallwitz, and E. Bi. 2003. The GAP activity of Msb3p and Msb4p for the Rab GTPase Sec4p is required for efficient exocytosis and actin organization. *J. Cell Biol.* 162:635–646. http://dx.doi.org/10.1083/jcb.200302038

Gautam, R., S. Chintala, W. Li, Q. Zhang, J. Tan, E.K. Novak, S.M. Di Pietro, E.C. Dell'Angelica, and R.T. Swank. 2004. The Hermansky-Pudlak syndrome 3 (cocoa) protein is a component of the biogenesis of lysosome-related organelles complex-2 (BLOC-2). *J. Biol. Chem.* 279:12935–12942. http://dx.doi.org/10.1074/jbc.M311311200

Gerondopoulos, A., L. Langemeyer, J.-R. Liang, A. Linford, and F.A. Barr. 2012. BLOC-3 mutated in Hermansky-Pudlak syndrome is a Rab32/38 guanine nucleotide exchange factor. *Curr. Biol.* 22:2135–2139. http://dx.doi.org/10.1016/j.cub.2012.09.020

Ghiani, C.A., and E.C. Dell'Angelica. 2011. Dysbindin-containing complexes and their proposed functions in brain: from zero to (too) many in a decade. *ASN Neuro*. 3.

Haas, A.K., E. Fuchs, R. Kopajtich, and F.A. Barr. 2005. A GTPase-activating protein controls Rab5 function in endocytic trafficking. *Nat. Cell Biol.* 7:887–893. http://dx.doi.org/10.1038/ncb1290

Hayes, M.J., K. Bryon, J. Satkurunathan, and T.P. Levine. 2011. Yeast homologues of three BLOC-1 subunits highlight KxDL proteins as conserved interactors of BLOC-1. *Traffic*. 12:260–268. http://dx.doi.org/10.1111/j.1600-0854.2010.01151.x

Henne, W.M., N.J. Buchkovich, and S.D. Emr. 2011. The ESCRT pathway. *Dev. Cell*. 21:77–91. http://dx.doi.org/10.1016/j.devcel.2011.05.015

Huotari, J., and A. Helenius. 2011. Endosome maturation. *EMBO J.* 30:3481–3500. http://dx.doi.org/10.1038/emboj.2011.286

Hutagalung, A.H., and P.J. Novick. 2011. Role of Rab GTPases in membrane traffic and cell physiology. *Physiol. Rev.* 91:119–149. http://dx.doi.org/10.1152/physrev.00059.2009

Janke, C., M.M. Magiera, N. Rathfelder, C. Taxis, S. Reber, H. Maekawa, A. Moreno-Borchart, G. Doenges, E. Schwob, E. Schiebel, and M. Knop. 2004. A versatile toolbox for PCR-based tagging of yeast genes: new fluorescent proteins, more markers and promoter substitution cassettes. *Yeast*. 21:947–962. http://dx.doi.org/10.1002/yea.1142

Kloer, D.P., R. Rojas, V. Ivan, K. Moriyama, T. van Vlijmen, N. Murthy, R. Ghirlando, P. van der Sluijs, J.H. Hurley, and J.S. Bonifacino. 2010. Assembly of the biogenesis of lysosome-related organelles complex-3 (BLOC-3) and its interaction with Rab9. *J. Biol. Chem.* 285:7794–7804. http://dx.doi.org/10.1074/jbc.M109.069088

Krogan, N.J., G. Cagney, H. Yu, G. Zhong, X. Guo, A. Ignatchenko, J. Li, S. Pu, N. Datta, A.P. Tikuisis, et al. 2006. Global landscape of protein complexes in the yeast *Saccharomyces cerevisiae*. *Nature*. 440:637–643. http://dx.doi.org/10.1038/nature04670

Lachmann, J., C. Ungermann, and S. Engelbrecht-Vandré. 2011. Rab GTPases and tethering in the yeast endocytic pathway. *Small GTPases*. 2:182–186. http://dx.doi.org/10.4161/sgtp.2.3.16701

Lachmann, J., F.A. Barr, and C. Ungermann. 2012. The Msb3/Gyp3 GAP controls the activity of the Rab GTPases Vps21 and Ypt7 at endosomes and vacuoles. *Mol. Biol. Cell*. 23:2516–2526. http://dx.doi.org/10.1091/mbc.E11-12-1030

Lee, H.H., D. Nemecek, C. Schindler, W.J. Smith, R. Ghirlando, A.C. Steven, J.S. Bonifacino, and J.H. Hurley. 2012. Assembly and architecture of biogenesis of lysosome-related organelles complex-1 (BLOC-1). *J. Biol. Chem.* 287:5882–5890. http://dx.doi.org/10.1074/jbc.M111.325746

Léon, S., Z. Erpapazoglou, and R. Haguenauer-Tsapis. 2008. Ear1p and Ssh4p are new adaptors of the ubiquitin ligase Rsp5p for cargo ubiquitylation and sorting at multivesicular bodies. *Mol. Biol. Cell*. 19:2379–2388. http://dx.doi.org/10.1091/mbc.E08-01-0068

Lin, C.H., J.A. MacGurn, T. Chu, C.J. Stefan, and S.D. Emr. 2008. Arrestin-related ubiquitin-ligase adaptors regulate endocytosis and protein turnover at the cell surface. *Cell*. 135:714–725. http://dx.doi.org/10.1016/j.cell.2008.09.025

Liu, W., R. Duden, R.D. Phair, and J. Lippincott-Schwartz. 2005. ArfGAP1 dynamics and its role in COPI coat assembly on Golgi membranes of living cells. *J. Cell Biol.* 168:1053–1063. http://dx.doi.org/10.1083/jcb.200410142

Martina, J.A., K. Moriyama, and J.S. Bonifacino. 2003. BLOC-3, a protein complex containing the Hermansky-Pudlak syndrome gene products HPS1 and HPS4. *J. Biol. Chem.* 278:29376–29384. http://dx.doi.org/10.1074/jbc.M301294200

Mullin, A.P., A. Gokhale, J. Larimore, and V. Faundez. 2011. Cell biology of the BLOC-1 complex subunit dysbindin, a schizophrenia susceptibility gene. *Mol. Neurobiol.* 44:53–64. http://dx.doi.org/10.1007/s12035-011-8183-3

Nazarian, R., J.M. Falcón-Pérez, and E.C. Dell'Angelica. 2003. Biogenesis of lysosome-related organelles complex 3 (BLOC-3): a complex containing the Hermansky-Pudlak syndrome (HPS) proteins HPS1 and HPS4. *Proc. Natl. Acad. Sci. USA*. 100:8770–8775. http://dx.doi.org/10.1073/pnas.1532040100

Newell-Litwa, K., G. Salazar, Y. Smith, and V. Faundez. 2009. Roles of BLOC-1 and adaptor protein-3 complexes in cargo sorting to synaptic vesicles. *Mol. Biol. Cell*. 20:1441–1453. http://dx.doi.org/10.1091/mbc.E08-05-0456

Nickerson, D.P., M.R.G. Russell, S.-Y. Lo, H.C. Chapin, J.M. Milnes, and A.J. Merz. 2012. Termination of isoform-selective Vps21/Rab5 signaling at endolysosomal organelles by Msb3/Gyp3. *Traffic*. 13:1411–1428. http://dx.doi.org/10.1111/j.1600-0854.2012.01390.x

Nikko, E., J.A. Sullivan, and H.R.B. Pelham. 2008. Arrestin-like proteins mediate ubiquitination and endocytosis of the yeast metal transporter Smf1. *EMBO Rep.* 9:1216–1221. http://dx.doi.org/10.1038/embor.2008.199

Nordmann, M., M. Cabrera, A. Perz, C. Bröcker, C.W. Ostrowicz, S. Engelbrecht-Vandré, and C. Ungermann. 2010. The Mon1-Ccz1 complex is the GEF of the late endosomal Rab7 homolog Ypt7. *Curr. Biol.* 20:1654–1659. http://dx.doi.org/10.1016/j.cub.2010.08.002

Ostrowicz, C.W., C. Bröcker, F. Ahnert, M. Nordmann, J. Lachmann, K. Peplowska, A. Perz, K. Auffarth, S. Engelbrecht-Vandré, and C. Ungermann. 2010. Defined subunit arrangement and Rab interactions are required for functionality of the HOPS tethering complex. *Traffic*. 11:1334–1346. http://dx.doi.org/10.1111/j.1600-0854.2010.01097.x

Pan, X., P. Roberts, Y. Chen, E. Kvam, N. Shulga, K. Huang, S. Lemmon, and D.S. Goldfarb. 2000. Nucleus-vacuole junctions in *Saccharomyces cerevisiae* are formed through the direct interaction of Vac8p with Nvj1p. *Mol. Biol. Cell*. 11:2445–2457.

Popovic, D., M. Akutsu, I. Novak, W. Harper, C. Behrends, and I. Dikic. 2012. Rab GAPs in Autophagy: regulation of endocytic and autophagy pathways by direct binding to human ATG8 modifiers. *Mol. Cell. Biol.* 32:1733–1744. http://dx.doi.org/10.1128/MCB.06717-11

Poteryaev, D., S. Datta, K. Ackema, M. Zerial, and A. Spang. 2010. Identification of the switch in early-to-late endosome transition. *Cell*. 141:497–508. http://dx.doi.org/10.1016/j.cell.2010.03.011

Puig, O., B. Rutz, B.G. Luukkonen, S. Kandels-Lewis, E. Bragado-Nilsson, and B. Séraphin. 1998. New constructs and strategies for efficient PCR-based gene manipulations in yeast. *Yeast*. 14:1139–1146. http://dx.doi.org/10.1002/(SICI)1097-0061(19980915)14:12<1139::AID-YEA306>3.0.CO;2-B

Raposo, G., and M.S. Marks. 2007. Melanosomes—dark organelles enlighten endosomal membrane transport. *Nat. Rev. Mol. Cell Biol.* 8:786–797. http://dx.doi.org/10.1038/nrm2258

Reggiori, F., and H.R. Pelham. 2001. Sorting of proteins into multivesicular bodies: ubiquitin-dependent and -independent targeting. *EMBO J.* 20:5176–5186. http://dx.doi.org/10.1093/emboj/20.18.5176

Reggiori, F., M.W. Black, and H.R. Pelham. 2000. Polar transmembrane domains target proteins to the interior of the yeast vacuole. *Mol. Biol. Cell*. 11:3737–3749.

Rink, J., E. Ghigo, Y. Kalaidzidis, and M. Zerial. 2005. Rab conversion as a mechanism of progression from early to late endosomes. *Cell*. 122:735–749. http://dx.doi.org/10.1016/j.cell.2005.06.043

Rivera-Molina, F.E., and P.J. Novick. 2009. A Rab GAP cascade defines the boundary between two Rab GTPases on the secretory pathway. *Proc. Natl. Acad. Sci. USA*. 106:14408–14413. http://dx.doi.org/10.1073/pnas.0906536106

Rodriguez-Fernandez, I.A., and E.C. Dell'Angelica. 2009. A data-mining approach to rank candidate protein-binding partners-The case of biogenesis of lysosome-related organelles complex-1 (BLOC-1). *J. Inherit. Metab. Dis.* 32:190–203. http://dx.doi.org/10.1007/s10545-008-1014-7

Salazar, G., B. Craige, M.L. Styers, K.A. Newell-Litwa, M.M. Doucette, B.H. Wainer, J.M. Falcon-Perez, E.C. Dell'Angelica, A.A. Peden, E. Werner, and V. Faundez. 2006. BLOC-1 complex deficiency alters the targeting of adaptor protein complex-3 cargoes. *Mol. Biol. Cell*. 17:4014–4026. http://dx.doi.org/10.1091/mbc.E06-02-0103

Salazar, G., S. Zlatic, B. Craige, A.A. Peden, J. Pohl, and V. Faundez. 2009. Hermansky-Pudlak syndrome protein complexes associate with

phosphatidylinositol 4-kinase type II alpha in neuronal and non-neuronal cells. *J. Biol. Chem.* 284:1790–1802. http://dx.doi.org/10.1074/jbc.M805991200

Schu, P.V., K. Takegawa, M.J. Fry, J.H. Stack, M.D. Waterfield, and S.D. Emr. 1993. Phosphatidylinositol 3-kinase encoded by yeast VPS34 gene essential for protein sorting. *Science*. 260:88–91. http://dx.doi.org/10.1126/science.8385367

Seaman, M.N.J., M.E. Harbour, D. Tattersall, E. Read, and N. Bright. 2009. Membrane recruitment of the cargo-selective retromer subcomplex is catalysed by the small GTPase Rab7 and inhibited by the Rab-GAP TBC1D5. *J. Cell Sci.* 122:2371–2382. http://dx.doi.org/10.1242/jcs.048686

Shi, Y., C.J. Stefan, S.M. Rue, D. Teis, and S.D. Emr. 2011. Two novel WD40 domain-containing proteins, Ere1 and Ere2, function in the retromer-mediated endosomal recycling pathway. *Mol. Biol. Cell*. 22:4093–4107. http://dx.doi.org/10.1091/mbc.E11-05-0440

Straub, R.E., Y. Jiang, C.J. MacLean, Y. Ma, B.T. Webb, M.V. Myakishev, C. Harris-Kerr, B. Wormley, H. Sadek, B. Kadambi, et al. 2002. Genetic variation in the 6p22.3 gene DTNBP1, the human ortholog of the mouse dysbindin gene, is associated with schizophrenia. *Am. J. Hum. Genet.* 71:337–348. http://dx.doi.org/10.1086/341750

Sung, M.-K., and W.-K. Huh. 2007. Bimolecular fluorescence complementation analysis system for in vivo detection of protein-protein interaction in *Saccharomyces cerevisiae*. *Yeast*. 24:767–775. http://dx.doi.org/10.1002/yea.1504

Wei, M.L. 2006. Hermansky-Pudlak syndrome: a disease of protein trafficking and organelle function. *Pigment Cell Res.* 19:19–42. http://dx.doi.org/10.1111/j.1600-0749.2005.00289.x

Yang, Q., X. He, L. Yang, Z. Zhou, A.R. Cullinane, A. Wei, Z. Zhang, Z. Hao, A. Zhang, M. He, et al. 2012. The BLOS1-interacting protein KXD1 is involved in the biogenesis of lysosome-related organelles. *Traffic*. 13:1160–1169. http://dx.doi.org/10.1111/j.1600-0854.2012.01375.x